Hindawi Publishing Corporation
ISRN Electronics
Volume 2013, Article ID 652587, 6 pages
http://dx.doi.org/10.1155/2013/652587

Research Article

Modeling of Electronic Transport through Metal/Polymer Interfaces in Thin Film Transistors

S. Alborghetti and P. Stamenov

School of Physics and CRANN, Trinity College Dublin, Dublin 2, Ireland

Correspondence should be addressed to S. Alborghetti; alborgs@tcd.ie

Received 29 November 2012; Accepted 16 January 2013

Academic Editors: R. Luzzi, L.-F. Mao, Y. Takahashi, P. Wachulak, and Y.-H. Wang

We report on the modeling of electrical characteristics and contact-related effects of organic thin film transistors. An equivalent circuit is employed to simulate the electrical behavior of the devices. We suggest that, at low temperature, tunneling is the dominant mechanism of charge carrier injection, originating the nonlinearities often observed in these devices. The temperature dependence of the output characteristics is due to the fraction of carriers that are injected, via the competing mechanism of thermal activation, above the interface energy barrier at metal/organic contacts. The model successfully reproduces the electrical characteristics of P3HT polymeric transistors and allows for the decoupling and the study of the temperature dependence of the charge conduction through the organic channel.

1. Introduction

Research into solution processable organic electronics has been a vibrant field of research over the last three decades. Many studies have focused on the realization of devices made with conjugated polymers due to the availability of simple deposition techniques to process these materials. While not destined to replace silicon-based technologies, they promise the advent of fully flexible devices for logic circuits, matrix displays, and photovoltaic cells. A common trait of polymer-based devices is that their performances critically depend on the efficiency with which charge carriers move within the conjugated material. Research efforts have been devoted to the development of high mobility polymers. Maximum mobilities of order $0.1\,\mathrm{cm^2V^{-1}s^{-1}}$ are found in thin films of polythiophene derivatives having enhanced interchain ordering [1]. This is about 4 orders of magnitude smaller than crystalline silicon, but similar to amorphous silicon. The low mobilities will naturally restrict applications to low frequency electronics.

The problem of contact resistance in hybrid organic devices has recently been recognized as a major issue too. At the earlier stages of research in this area, the conductivity of the available media has been low, so that the device output current has in most cases been entirely limited by the organic channel resistance. As new materials with improved mobility have been synthetized, limitations by contact resistance are getting more and more crucial. Reinforcing this concern, modern devices are typically designed with much shorter channel length. As an example, in field effect transistors (FETs), this is motivated by the necessity to obtain switching speeds and drive currents that meet the requests of applications. In these circumstances the contact effects are expected to heavily affect the performance of the devices. In transistors, the drain currents scales with the transistor width, as the actual contact resistance r_C is inversely proportional to the channel width W ($r_C \propto W^{-1}$). Therefore, it is convenient to use the product of contact resistance and channel width, $R_C = r_C W$, as a measure of the contact resistance. Contact resistance at a metal-organic interface is usually detected to be in the range of $10\,\mathrm{k\Omega\,cm}$–$10\,\mathrm{M\Omega\,cm}$ [2, 3]. In inorganic devices; for example, in FETs, source and drain contacts are typically optimized by selective semiconductor doping, which leads to much lower values, and so it is expected that

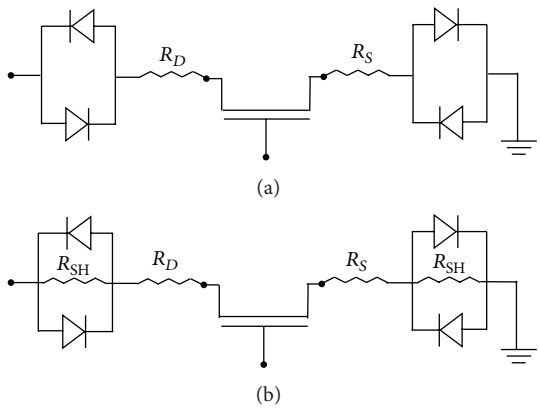

Figure 1: (a) simplified effective circuit representing an organic channel FET transistor and a more complicated version of the same including additional current injection mechanisms (b).

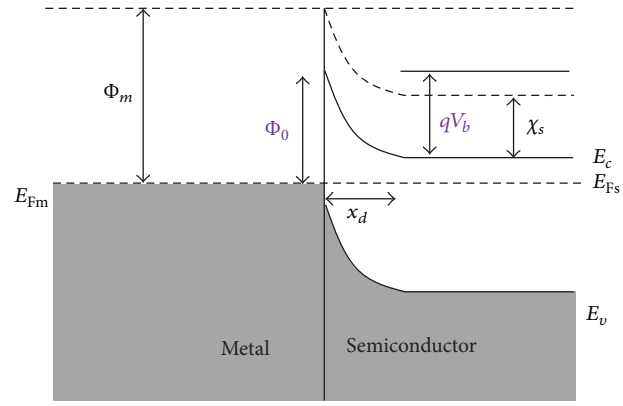

Figure 2: A schematic energy diagram of a Schottky contact.

contact effects will be dominating mostly in short channel hybrid devices. As the contact resistance is expected to be independent of the channel length L, the actual channel resistance scales with L. Assuming a linear dependence, for simplicity, when the channel resistance $R_{Ch} = L/W\mu en$ (where n is the density of charges per unit area and $W$is the channel width) equals the contact resistance R_C, the contacts and the channel equally contribute to the total device resistance. A critical channel length $L_{Cr} = \mu enR_C$ can be defined, for which $WR_{Ch} = R_C$. In an FET, it is only for longer channel devices that clean transistor behavior can be expected. On the other side, when the channel is shorter than the critical value, the drain bias will mainly drop over the contact regions. Following [4], for polythiophenes ($\mu \approx 10^{-2}\,\mathrm{cm^2V^{-1}s^{-1}}$, $R_C \approx 50\,\mathrm{k\Omega\,cm}$, and $n \approx 2 \cdot 10^{12}\,\mathrm{cm^{-2}}$) $L_{Cr} \approx 2\,\mu\mathrm{m}$.

The main effect of the contact resistance is a nonlinear increase of the output characteristics at increasing drain voltages. In order to improve the fit to this type of experimental data and to simulate the non-linear $I:V$ characteristics of pentacene FETs, device response was modeled with a circuit consisting of an ohmic FET channel having a pair of antiparallel Schottky diodes connected to the access resistors [5], as shown in Figure 1(a). Two diodes in parallel are employed so as to obtain symmetric current-voltage characteristics. The diodes are in series with the contact resistance of source and drain and the intrinsic channel resistance. Whereas the pair of diodes is enough to simulate the nonlinearity, an accurate fit to the data over a large range of voltage is only achieved by modeling the injection process with a shunt resistor R_{sh} in parallel with the Schottky diodes [3, 6] (Figure 1(b)). At low drain biases each Schottky diode contributes to the current conduction only to a very little extent; hence the FET would consist of a pair of shunt resistors in series with the contacts and the channel. In this region of device bias the total device resistance is dominated by the high value shunt resistance, the current-voltage characteristics are linear, and the conductance is severely limited. When the drain bias exceeds the diode turn-on voltage, the FET is a combination of the contact resistance and the intrinsic channel resistance. Such representation is not purely empirical; high contact resistances often originate from the formation of a potential barrier at the organic-metal interface. The common way to describe it is that of a metal/semiconductor contact (Schottky contact). In a simple view the barrier height is given by the difference between the metal work function Φ_m and the semiconductor HOMO or LUMO level (Figure 2). Good contacts are expected to occur when Φ_m is close to one of these levels. In the reverse situation, a potential barrier forms at the interface, leading to poor charge injection. Even though this simplification helps to comprehend the origin of the interface barrier, this approximation is often not valid, especially when the interface exhibits an additional dipole barrier that tends to lower the metal work function. As a consequence, even when the nominal work functions of the materials do match, the interface barrier height remains high, as, for example, in [7, 8], for polymers and pentacene on gold. Here a large interface dipole is attributed to the change of the surface dipole of the metal following the adsorption of organic molecules. As a metal surface is characterized by an electron density tailing from the free surface into vacuum, adsorbed molecules tend to compress these electrons, eventually inducing a large interface dipole density and decreasing the work function of the metal. This leads to an increase in the energy difference between the metal Fermi level and the highest occupied molecular orbital of the organic film. As a result, the hole interface barrier is enlarged.

The effects of temperature, which are of key importance for charge injection, have been studied in [9], which concludes that diffusion-limited thermionic emission on top of a potential barrier at the semiconductor-metal contact is the dominant process for injection of carriers in organic transistors. Similarly, the contact resistance has been interpreted in terms of thermionic emission in [3, 5, 10, 11]. The formation of an interface Schottky barrier is indeed well documented by photoemission measurements [12, 13]. The tuning of the Schottky energy barriers by attaching oriented dipoles layers on top of the metal contacts has also been performed in [14], which undoubtedly proves the presence of these potential barriers. Using an atomic force microscope tip to sense the potential along the channel of a transistor [15] (noncontact

scanning probe potentiometry), an analysis of organic FETs has been performed in [4], revealing the potential profile inside operating devices, with high spatial resolution. It has been found that for electrode-polymer combinations that form bad contacts, with a relatively large Schottky barrier, charge injection across the barrier constitutes the main obstacle leading to high contact resistances, with a voltage drop at the source electrode much higher than that at the drain. However, for good contacts combination with low Schottky barrier, the voltage drop was found to be of comparable magnitude at both electrodes. This is understood as a consequence of bulk transport in the polymer through a very narrow depleted region in the vicinity of the contacts, which dominates the contact resistance for low Schottky barrier, leading to a symmetric voltage drop. As a general consequence, contact resistance is not entirely accounted by diffusion-limited thermionic emission, but alternative injection mechanisms also play a dominant role [16, 17]. It has been proposed that thermally assisted tunneling [18] and thermally assisted injection [19] occur from a continuum of states in the metal into localized states of an organic media, whose distribution is smeared at increasing temperature, resulting in a strongly temperature-dependent carrier injection. As the depletion layer is very narrow, of order few nanometers, and the electric fields can be very large in short channel devices, tunneling can well play a dominant role.

Given the barrier shape, the expression of the tunneling current is obtained by the product of the carrier charge q, the velocity v_R, the density of carriers n, and the tunneling probability Θ; as $J_n = qnv_r\Theta$. The velocity equals the Richardson velocity, the velocity with which on average the carriers approach the barrier $v_R = \sqrt{k_B T/2\pi m_c^*}$, where m_c^* is the effective mass. For a rectangular, or close to symmetric triangular, barrier ϕ_b the current is given by

$$J_n = qv_R N_c \exp\left(-\frac{4}{3}\frac{\sqrt{2m_c^*}}{\hbar}\sqrt{q\phi_b}x_d\right)\left[\exp\left(\frac{qV_a}{\gamma kT}\right)-1\right], \quad (1)$$

where γ is the customary ideality factor, which is used as a "fudge" factor, hiding a number of different competing physical mechanisms that are responsible for deviations from the nominal thermal activation scale. The tunneling current shows explicit temperature dependence only in the applied voltage-dependent part of the above equation; hence for low biases it is often approximated as temperature independent. The term $\propto \sqrt{T}$ from v_R is also typically neglected.

2. Modeling Principles

Figure 3 shows a representative $I:V$ characteristic of a polymeric transistor from [20], prepared with gold electrodes and P3HT organic spacer; the non-linearity is enhanced by having measured the curve at a low temperature $T = 7$ K and short channel length of 80 nm, which results in contact-dominated devices. The measured curve reminds of the response characteristic of a pair of tunneling diodes connected to the access resistors of an FET, as in Figure 4(a). Attempts to fit the curves have been successful by using an

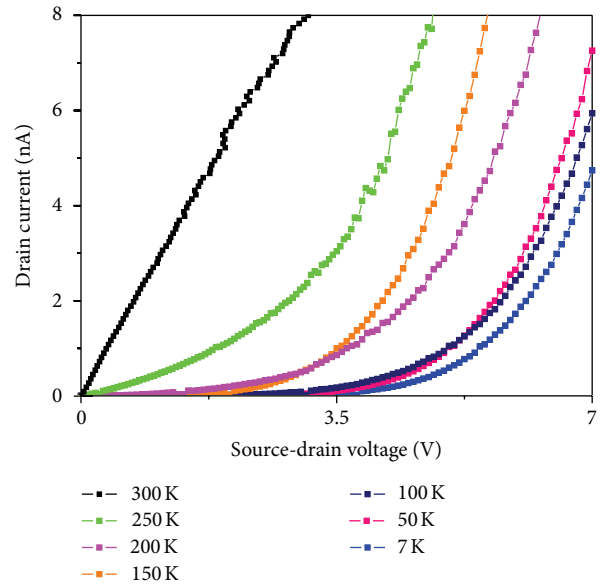

Figure 3: A representative set of $I:V$ characteristics of P3HT organic FET at various temperatures, as indicated in the legend.

expression accounting for initial non-linear voltage drops at the tunneling contacts $V_{t|D}$ and $V_{t|S}$, the subscripts D and S stand for drain and source, followed by a voltage drop adjacent to the source-drain contacts V_D and V_S (transport in the depleted region) and dissipation across the organic channel, which was assumed to be intrinsically ohmic, with resistance R_{Ch}. A system of equation can be defined to describe the physical picture:

$$\begin{aligned} V &= V_{t|D} + V_D + V_{\mathrm{Ch}} + V_S + V_{t|S}, \\ V_{t|D} &= \phi_D \ln\left(\frac{I - I_{\mathrm{off}}}{A_D}\right) - \phi_D \ln\left(\frac{I_{\mathrm{off}}}{A_D}\right), \\ V_{\mathrm{Ch}} &= (I - I_{\mathrm{off}})\, R_{\mathrm{Ch}}, \\ V_{t|S} &= \phi_S \ln\left(\frac{-I + I_{\mathrm{off}}}{A_S}\right) - \phi_S \ln\left(\frac{I_{\mathrm{off}}}{A_S}\right). \end{aligned} \quad (2)$$

Here the first equation includes the fact that the whole voltage drop across the device is given by the aforementioned terms; the second and the fourth express the nonlinear dependence of the current on the applied bias in tunneling contacts; A_D and A_S are the effective contact area, ϕ_D and ϕ_S the barrier activation voltage scale (for reasons of simplicity hereafter just referred to as barrier height, despite the fact that it may, and often does, depend in magnitude on the barrier width, as well as on the presence of additional transport (current limiting) mechanisms), and I_{off} a current offset. Although somewhat counterintuitive, expressing the equation in the $V:I$ form is convenient, as the equations describing the two contact regions are solvable in terms of the individual voltage drops, and the equation for the overall potential drop across the structure is a simple linear summation. The same physical model is equally well describable in terms of current; however, the mathematical formulation

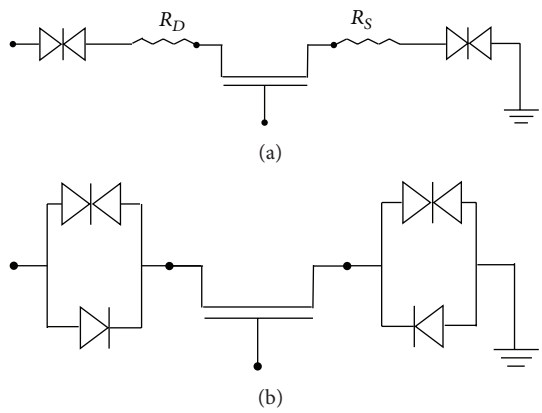

Figure 4: A simplified effective circuit used to model the polymer-FETs' $I:V$ characteristics (a) and the physical version of the same, depicting explicitly the competing processes of thermionic emission over tunneling through the contact barriers (b).

is rather heavy and can involve special functions and/or integral forms that are not readily available in common data processing and fitting packages, such as Origin. The transition from conventional vertical regression to a horizontal one does not have a significant implication on the convergence properties of the process, apart from some extreme cases of very low signal-to-noise ratios in the experimental current measurements. This system can be combined in an equation to be used for the fitting process as

$$V = \begin{cases} V_D + IR_{\mathrm{Ch}} + \phi_D \ln\left[\dfrac{A_D + I + A_D\left(e^{-V_D/\phi_D} - 1\right)}{A_D}\right] \\ \quad -\phi_D \ln\left[\dfrac{A_D + A_D\left(e^{-V_D/\phi_D} - 1\right)}{A_D}\right], \\ \qquad\qquad \text{if } I > 0, \\ V_S - IR_{\mathrm{Ch}} + \phi_S \ln\left[\dfrac{A_S - I + A_S\left(e^{-V_S/\phi_S} - 1\right)}{A_S}\right] \\ \quad -\phi_S \ln\left[\dfrac{A_S + A_S\left(e^{-V_S/\phi_S} - 1\right)}{A_S}\right], \\ \qquad\qquad \text{if } I < 0, \\ 0, \qquad\qquad \text{otherwise.} \end{cases} \tag{3}$$

Each contact was permitted to have a different barrier height $\phi_{D|S}$, active area $A_{D|S}$, and constant voltage drop $V_{D|S}$. The voltage drop $V_{D|S}$ at the contacts, in fact, resembles the initial nonlinear contribution of thermionic emission over the barrier, which adds in parallel with the dominant tunneling contribution. These two terms could be in principle separated, but it would require a greatly complicated system of model equations. Hence, it is convenient simply to add a contact voltage offset; in fact the thermionic emission only shifts toward higher bias the turn-on voltage of the tunneling diode, when the two mechanisms occur in parallel.

No explicit temperature dependence appears in the expression describing the tunneling current across a barrier. To account for the shift toward higher biases of the turn-on voltage of the $I:V$ characteristics of [20] (the voltage at which the current starts being efficiently injected inside the semiconductor), we propose a new equivalent circuit. This model consists of a tunneling contact in parallel with a Schottky diode, connected to each terminal of the FET (Figure 4(b)). It should be noted that devices cannot be modeled simply by two back-to-back Schottky diodes because, in that case, one would always be in reverse bias, hence saturating and limiting the current to very low values. An exponential increase is observed instead, typically attributable to tunneling. The question arising is where is the temperature dependence of the curves (and the temperature dependence of the voltage drop at the interface) coming from? To answer this question, we need to consider that, in general terms, carriers can be injected both across and above an energy barrier, respectively, via tunneling and via thermally activation (excitation); the two mechanisms are typically contributing to a different extent. Strong temperature dependence is a characteristic of (and normally associated with) thermionic emission over the barrier. It is evident that our curves shift toward larger bias on lowering the temperature, indicating that thermal excitation plays a significant role. The circuit of Figure 4(b) includes the fact that injection can occur in parallel via these two principal mechanisms through the contacts. For each applied voltage, one Schottky diode will be found in reverse bias, hence limiting the overall current flowing in the device. Current can be injected efficiently via the competing mechanism of tunneling only at high enough voltages. Therefore, at low biases, the reverse Schottky diode is shorting the pair of parallel contacts, absorbing all the current, but resulting in only a small voltage drop (due to its non-linear characteristic). When the Schottky diodes reach saturation (in reverse bias), the current can start flowing through the tunneling contact (as per the increased differential resistance of the Schottky component), and an exponential increase of the current is expected. The saturation voltage of the Schottky diodes depends exponentially on temperature, and it is larger for lower temperature. This explains why the $I:V$ curves of [20] essentially shift toward higher biases. A further temperature dependence comes from the change in resistance of the active channel; the term IR_{Ch} in this device is masked, at low temperature, by the contact effects, but it can be extracted at each temperature using the set of equations shown above, hence studying the temperature dependence of conduction in the organic material. The complexity of the extended model system, corresponding to Figure 4(b), (6 non-linear equations) would not allow extracting meaningful, linearly independent fitting parameters from just a family of close-to-exponential curves. Hence, the simpler circuit of Figure 4(a), consisting of tunneling contacts and access resistors, is more suitable for analyzing organic transistors. Here the temperature dependence can be attributed to the resistors in the effective circuit, with no concern or discrimination of the physical origin of the mechanisms. This allows the extraction of the activation potential barrier and of the channel resistance over a large temperature range.

The $V:I$ curves are well fitted by exponential plus linear terms corresponding to tunneling contact in series with

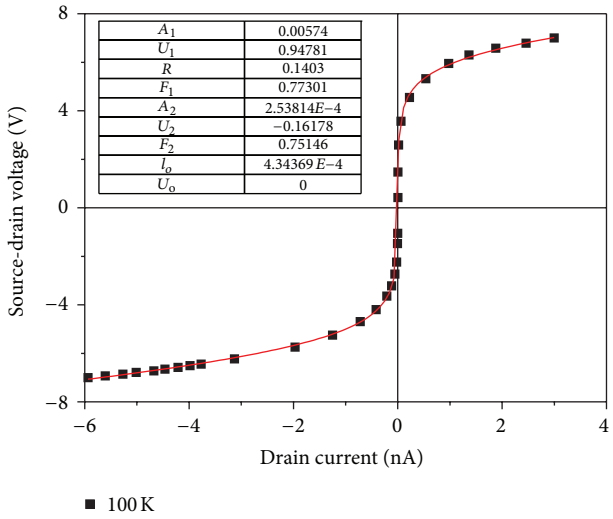

Figure 5: Simulation/fitting obtained with the parameters in the inset. 1 and 2 indicate source and drain, R is expressed in GΩ. F indicates the barrier activation voltage. The experimental data were taken at 100 K and −50 V applied on the gate.

ohmic channel (Figure 5). In this particular device, consisting of CoFe drain and source contacts and P3HT channel, the barrier activation voltage was slightly asymmetric on the two sides of the junction. In the plot, a value of 0.77 V and 0.75 V was found at source and drain, respectively, which is likely due to slight asymmetry of contact-interface morphology [21]. By modeling the device with this equivalent circuit, the channel resistance can also be extracted and used to study the effect of the gate field on the organic channel conductance. In Figure 6 we have recorded the electrical characteristics at 7 K as a function of applied gate voltage for the same device. The observed response to a local electric field exhibits the general behavior of a hole transporting system, in which the drain current is enhanced by negative gate biases. The application of positive gate voltages shuts down the conduction in the channel.

The extracted activation voltage, which is directly related to the barrier height, can also be extracted for different combination of polymer/metal interfaces. In Table 1 we derived the useful indication that the barrier activation voltage neither shows a direct relation with the presence/absence of an interface oxide nor with the difference of work function of the materials on the two sides of the junction (as in a simple rigid-band picture) [20]. Rather, some mechanisms exist so that the Fermi level is pinned at the interface and the effective metal work function shifts toward lower values [7, 20, 22].

3. Discussion

The mechanisms of thermionic emission and tunneling typically occur in parallel, as competing processes for carrier injection across a contact interface, but thermal activation is expected to dominate at high temperature and tunneling at low temperature. In both processes the electric field dependence is exponential (even though one diode is in reverse, hence is a decreasing exponential) and they can hardly be distinguished with an analysis such as the one described above. However, by using a simplified equivalent circuit model and a corresponding system of equations, it is possible to fit the $I:V$ characteristics of organic FET devices, so as to extract both of the resistance of the organic channel and the activation voltage scale of the barriers. For practical engineering scaling reasons, it is critical to be able to distinguish the channel and the contact contributions to the overall device resistance as, especially in short channel devices, the contacts can play a dominant role and mask the more interesting intrinsic organic behavior. It is noteworthy that the resistance of the organic channel can be extracted at each temperature using the set of equations shown, leading to the possibility to study, also, the temperature dependence of the conductivity in the organic material. This, in turn, can provide some indications about the conduction mechanisms within the semiconductor itself. We recall that the process of carrier migration in organic material is still a debated subject, and revealing its temperature dependence can be of great importance. Also, the activation voltage of the barrier existing

Table 1: The extracted value of the barrier activation voltage (~ barrier height) for the source and drain electrodes is given, for the set of contact material studied in this work.

Electrode material	Φ_s (eV)	Φ_d (eV)
Au	0.84	0.68
CoFe/Al/Al_2O_3	0.84	0.85
CoFe/Al_2O_3 (as deposited)	0.79	0.66
CoFe/Al_2O_3 (natural oxidation)	0.73	0.58
NiFe	0.47	0.49
CoFe	0.70	0.80

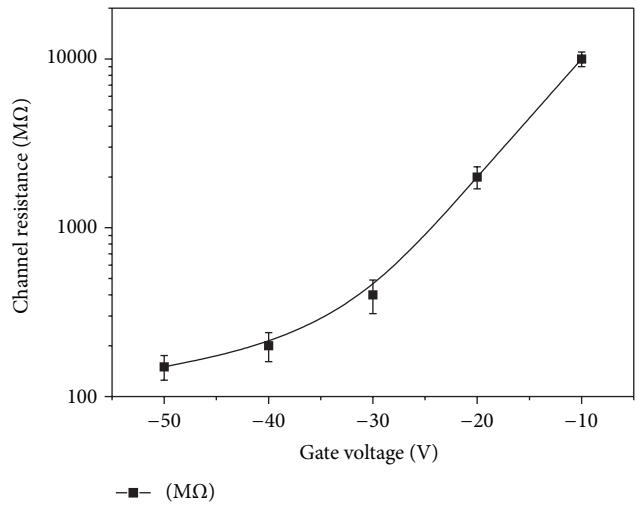

Figure 6: Plot of the organic channel resistance as a function of the applied gate voltage, at 7 K. As expected for hole conduction, the channel becomes more conductive at increasingly negative gate voltages.

at the contact can be successfully extracted. Intuitively there is no good reason why the contacts should have exactly the same active areas and barrier heights; in fact the fine structure of each electrode can affect the local morphology of the organic medium, which in turn affects the injecting barrier and the depleted region [22]. The electrodes within a device are nominally the same, but topological differences in, for example, spin-cast polymers, naturally occur.

In conclusion, with the model reported in this paper, it becomes possible to simulate the non-linearity of the electrical characteristics of organic thin film transistors and use it to extract useful parameter from the fitting of such curves, for investigating both contact effects and the transport mechanisms within the organic media itself.

Conflict of Interests

S. Alborghetti and P. Stamenov wish to state that they have no direct financial relations with any of the commercial entities mentioned in the paper, which may potentially lead to conflict of interests. Any references to commercial trademarks are included only in the interest of traceability of the materials and softwares used.

Acknowledgment

This research was supported by Science Foundation Ireland as part of the NISE project, Contract no. 10/IN1/I3002.

References

[1] Y. Y. Noh and H. Sirringhaus, "Ultra-thin polymer gate dielectrics for top-gate polymer field-effect transistors," *Organic Electronics*, vol. 10, no. 1, pp. 174–180, 2009.

[2] J. Zaumseil, K. W. Baldwin, and J. A. Rogers, "Contact resistance in organic transistors that use source and drain electrodes formed by soft contact lamination," *Journal of Applied Physics*, vol. 93, no. 10, pp. 6117–6124, 2003.

[3] P. V. Necliudov, M. S. Shur, D. J. Gundlach, and T. N. Jackson, "Contact resistance extraction in pentacene thin film transistors," *Solid-State Electronics*, vol. 47, no. 2, pp. 259–262, 2003.

[4] L. Bürgi, T. J. Richards, R. H. Friend, and H. Sirringhaus, "Close look at charge carrier injection in polymer field-effect transistors," *Journal of Applied Physics*, vol. 94, no. 9, pp. 6129–6137, 2003.

[5] P. V. Necliudov, M. S. Shur, D. J. Gundlach, and T. N. Jackson, "Modeling of organic thin film transistors of different designs," *Journal of Applied Physics*, vol. 88, no. 11, pp. 6594–6597, 2000.

[6] D. J. Gundlach, L. Zhou, J. A. Nichols, T. N. Jackson, P. V. Necliudov, and M. S. Shur, "An experimental study of contact effects in organic thin film transistors," *Journal of Applied Physics*, vol. 100, no. 2, Article ID 024509, 2006.

[7] N. Koch, A. Kahn, J. Ghijsen et al., "Conjugated organic molecules on metal versus polymer electrodes: demonstration of a key energy level alignment mechanism," *Applied Physics Letters*, vol. 82, no. 1, pp. 70–72, 2003.

[8] G. Horowitz, "Organic thin film transistors: from theory to real devices," *Journal of Materials Research*, vol. 19, no. 7, pp. 1946–1962, 2004.

[9] A. B. Chwang and C. Daniel Frisbie, "Field effect transport measurements on single grains of sexithiophene: role of the contacts," *Journal of Physical Chemistry B*, vol. 104, no. 51, pp. 12202–12209, 2000.

[10] R. A. Street and A. Salleo, "Contact effects in polymer transistors," *Applied Physics Letters*, vol. 81, no. 15, pp. 2887–2889, 2002.

[11] T. Li, J. W. Balk, P. P. Ruden, I. H. Campbell, and D. L. Smith, "Channel formation in organic field-effect transistors," *Journal of Applied Physics*, vol. 91, no. 7, p. 4312, 2002.

[12] I. H. Campbell, T. W. Hagler, D. L. Smith, and J. P. Ferraris, "Direct measurement of conjugated polymer electronic excitation energies using metal/polymer/metal structures," *Physical Review Letters*, vol. 76, no. 11, pp. 1900–1903, 1996.

[13] N. Nakanishi, K. Tada, M. Onoda, and H. Nakayama, "Electronic states at conducting polymer/conducting oxide interfaces observed using a low-energy photoelectron spectroscopic method," *Applied Physics Letters*, vol. 75, no. 2, pp. 226–228, 1999.

[14] I. H. Campbell, S. Rubin, T. A. Zawodzinski et al., "Controlling Schottky energy barriers in organic electronic devices using self-assembled monolayers," *Physical Review B*, vol. 54, no. 20, pp. R14321–R14324, 1996.

[15] K. Seshadri and C. D. Frisbie, "Potentiometry of an operating organic semiconductor field-effect transistor," *Applied Physics Letters*, vol. 78, no. 7, pp. 993–995, 2001.

[16] T. van Woudenbergh, P. W. M. Blom, M. C. J. M. Vissenberg, and J. N. Huiberts, "Temperature dependence of the charge injection in poly-dialkoxy-p-phenylene vinylene," *Applied Physics Letters*, vol. 79, no. 11, pp. 1697–1699, 2001.

[17] Y. Preezant and N. Tessler, "Self-consistent analysis of the contact phenomena in low-mobility semiconductors," *Journal of Applied Physics*, vol. 93, no. 4, p. 2059, 2003.

[18] M. A. Abkowitz, H. A. Mizes, and J. S. Facci, "Emission limited injection by thermally assisted tunneling into a trap-free transport polymer," *Applied Physics Letters*, vol. 66, no. 10, pp. 1288–1290, 1995.

[19] V. I. Arkhipov, E. V. Emelianova, Y. H. Tak, and H. Bässler, "Charge injection into light-emitting diodes: theory and experiment," *Journal of Applied Physics*, vol. 84, no. 2, pp. 848–856, 1998.

[20] S. Alborghetti, M. Coey, and P. Stamenov, "Dependence of charge carrier injection on the interface energy barrier in short-channel polymeric field effect transistors," *Applied Physics Letters*, vol. 100, no. 14, Article ID 143301, 4 pages, 2012.

[21] N. Koch, A. Elschner, J. Schwartz, and A. Kahn, "Organic molecular films on gold versus conducting polymer: influence of injection barrier height and morphology on current-voltage characteristics," *Applied Physics Letters*, vol. 82, no. 14, pp. 2281–2283, 2003.

[22] K. A. Singh, T. Young, R. D. McCullough, T. Kowaiewski, and L. M. Porter, "Planarization of polymeric field-effect transistors: improvement of nanomorphology and enhancement of electrical performance," *Advanced Functional Materials*, vol. 20, no. 14, pp. 2216–2221, 2010.